

Analysis on the accuracy of CT-guided radioactive I-125 seed implantation with 3D printing template assistance in the treatment of thoracic malignant tumors

Zhe Ji, Haitao Sun, Yuliang Jiang, Yi Chen, Fuxin Guo, Jinghong Fan and Junjie Wang*

Department of Radiation Oncology, Peking University Third Hospital, Beijing, China

*Corresponding author. Department of Radiation Oncology, Peking University Third Hospital, Beijing 100191, China. Email: junjiewang_edu@sina.cn
(Received 30 April 2021; revised 10 June 2021; editorial decision 9 July 2021)

ABSTRACT

This article analyzes the accuracy of needle track and dose of a 3-dimensional printing template (3DPT) in the treatment of thoracic tumor with radioactive I-125 seed implantation (RISI). A total of 28 patients were included. The technical process included: (i) preoperative CT positioning, (ii) preoperative planning design, (iii) 3DPT design and printing, (iv) 3DPT alignment, (v) puncture and seed implantation. The errors of needle position and dosimetric parameters were analyzed. A total of 318 needles were used. The mean errors in needle depth, needle insertion point, needle tip and needle angle were 0.52 ± 0.48 cm, 3.4 ± 1.7 mm, 4.4 ± 2.9 mm and $2.8 \pm 1.7^\circ$, respectively. The differences between actual needle insertion angle and needle depth and those designed in the preoperative were statistically significant ($p < 0.05$). The mean values of all the errors of the chest wall cases were smaller than those of the lungs, and the differences were statistically significant ($p < 0.05$). There was no significant difference between the D90 calculated in the postoperative plan and those designed in the preoperative and intraoperative plans ($p > 0.05$). Some dosimetric parameters of preoperative plans such as V100, V200, CI and HI were not consistent with that of preoperative plans, and the difference was statistically significant ($p < 0.05$). However, there were no statistical difference in the dosimetric parameters between the postoperative plans and intraoperative plans ($p > 0.05$). We conclude that for thoracic tumors, even under the guidance of 3DPT, there will be errors. The plan should be optimized in real time during the operation.

Keywords: 3D-printing template; radioactive seed implantation; thoracic tumor; error; dos

INTRODUCTION

Radioactive I-125 seed implantation (RISI) for the treatment of malignant tumors has the advantages of high local dose, minimal invasiveness and fewer complications. It is mostly used in other countries in the treatment of prostate cancer [1]. With the continuous exploration in clinical practice, RISI also played an increasingly important role in the local treatment and palliative treatment of various types of relapsed and refractory solid tumors [2–5]. The distribution of seed needles has a vital influence on the distribution, dosage and even curative effect of the seeds [6]. With the help of the Brachytherapy Treatment Planning System (BTPS), the appropriate needle track can be selected in the preoperative planning stage to make the seeds reasonably distributed. Thereby, the dose of the target zone can be optimized and the exposure

of the organs at risk (OAR) can be reduced [7]. However, due to the impact of tumor volume, shape and complex anatomical factors of the human body, the needle track designed by the preoperative plan is often complicated to achieve the required therapeutic dose. Furthermore, there is great uncertainty in the manual puncture relying solely on image guidance. The performance, experience and technical ability of the surgeon has a significant impact on the accuracy and safety of the operation. The effects are also uneven, which is not conducive to clinical promotion and standardization.

In recent years, the 3-Dimensional Printing Template (3DPT) technology has rapidly developed in the field of seed implantation. This technology can conform to the body's surface, and the guide column can control the needle's direction [8]. Multiple studies have

confirmed that RISI assisted by 3DPT can achieve individualized and precise treatment, and the postoperative dose better meets the design requirements of the preoperative plan [9, 10]. However, most studies only confirmed the accuracy of the dose and did not mention the accuracy of needle insertion. For chest lesions in particular, in addition to avoiding important organs and blood vessels during the puncture operation, there are also problems related to respiratory movement, which often leads to a complicated treatment plan for BTPS. It is difficult for the actual situation during and after the operation to be consistent with the preoperative plan. This study intends to perform error analysis on the puncture needle track and dosimetry of 3DPT-guided thoracic tumor RISI treatment to further clarify the accuracy of 3DPT-guided operation and to provide a reference for further optimization of the puncture guidance method and to improve the accuracy of RISI treatment.

MATERIALS AND METHODS

Software

The BTPS (model KL-SIRPS-3D; provided by Beijing Astro Technology Co., Ltd.) and the source data of the planned system were based on the American Association of Physicists in Medicine (AAPM) TG 43 and its updated files [11, 12]; The 3D imaging and reverse engineering software used was Magics 19.01 (Materialise, Belgium).

Hardware equipment

The equipment consisted of Computed Tomography (CT) (Brilliance Bigbore, Philips, Netherlands); A 3D printer (Shanghai Union Technology Corporation, RS6000), with a printing accuracy of 0.02–0.1 mm. The printing material was medical-grade light-curable resin (IMAGINE 8000) that adheres to the European EEC (European Communities) Standard; and I-125 seeds (6711_1985 type; HTA Co., Ltd.; half-life, 59.4 d). The dose rate constant was 0.965 cGy/(h·U) (6). The RISI equipment was from Mick Radio-Nuclear Instruments, Eckert & Ziegler BEBIG, USA.

Clinical data

A total of 28 patients with thoracic malignancies who received 3DPT assisted CT-guided RISI treatment in our department from December 2019 to December 2020 were included. All patients had complete imaging data, preoperative, intraoperative, postoperative plans and intraoperative operating data. All treated patients met the indication criteria for expert consensus of radioactive seed implantation [13]: (i) Patients with recurrence after surgery or external radiotherapy, or patients who refused surgery or external radiotherapy, tumor diameter ≤ 7 cm, (ii) clear pathological diagnosis, (iii) appropriate puncture track, (iv) no bleeding tendency or hypercoagulable state, (v) general physical condition was acceptable, such as Karnofsky Performance Score (KPS) > 70 points, (vi) the patient could tolerate radioactive seed implantation, (vii) the expected survival time was more than three months. All patients signed an informed consent form before treatment. The basic information of the patients, target lesions and preoperative plans are presented in Table 1.

Technical process of RISI treatment

Preoperative CT positioning

Two days before the operation, the patient was positioned according to the surgical position requirements. The position was then fixed with a negative pressure vacuum pad. The positioning laser line was used to mark the body surface projection of the tumor center layer on the patient's body surface. It was then marked with lead spots; a 4D-CT scan was used with a slice thickness of 2.5 mm. CT data were stored in Digital Imaging and Communications in Medicine (DICOM) format and transmitted to BTPS.

Preoperative planning design

BTPS, the Gross Tumor Volume (GTV) and surrounding OAR were outlined and the puncture needle track (needlepoint, angle and depth) was designed based on the Maximum Intensity Projection (MIP) images obtained by 4D-CT. The number of seeds was calculated to simulate the spatial distribution of seeds and to enable the dose to meet the prescription requirements.

The 3DPT design and printing

Firstly, a 3DPT virtual model with guideposts was generated according to the needle track distribution in BTPS, then the 3D model was smoothed and the printing range was set. The 3D model data were input into a 3D light-curing rapid prototyping machine (3D printer) to process an individualized 3DPT. The factors that needed to be considered during the design included the following: (i) the edge of the plate body should be at least 10 mm away from the edge of the guide hole to ensure the rigidity of the guide hole structure, (ii) the plate body should be designed to have structures with certain retention function, such as sternal notch, costal arch, etc., based on the shape of the body surface, (iii) the design of the reserved needle track. The reserved needle track is an additional needle track around the puncture guide column and is within 5–10 mm of the tumor edge. It only reserved a puncture hole, did not generate a guidepost and had no restriction on the direction of the puncture needle. This facilitated the flexible change and adjustment of the puncture needle position when the position of the lesion changed during the operation, (iv) the thickness of the 3DPT was 2.5 mm, and the length of the guide hole was 13 mm, which ensured that the needle insertion was accurately directed. The diameter of the seed needles was 1.3 mm, and the inner wall of the template guide hole was 1.4 mm in diameter, which ensured smooth insertion of the needle and no movement in the guide hole.

The 3DPT alignment

The patient was repositioned with the help of a negative pressure vacuum pad, positioning laser line and patient surface marking line, so that the patient's position was consistent with that at the time of positioning. The 3DPT was placed on the surface of the patient's treatment area and accurately aligned with the help of a positioning laser line. The patient's body surface marking line, the template coordinate line and the outer contour features of the body surface. A CT scan was performed to confirm the accuracy of the relative position between the template

Table 1. General information of patients and lesions

Characteristics	N	%
Gender		
Male	21	75.0
Female	7	25.0
Age (years old)	60 (20–79)	
KPS	80 (70–90)	
Primary disease		
Lung cancer	15	53.6
Head & neck cancer	3	10.7
Breast cancer	2	7.1
Esophageal cancer	1	3.6
Gastric cancer	1	3.6
Liver cancer	1	3.6
Colorectal cancer	1	3.6
malignant mesenchymal tumor	1	3.6
Sarcoma	1	3.6
Thyroid cancer	1	3.6
Renal cancer	1	3.6
Location of implantation		
Left upper lobe	3	10.7
Left lower lobe	4	14.3
Right upper lobe	3	10.7
Right lower lobe	9	32.1
Right middle lobe	1	3.6
Chest wall	8	28.6
Lesion size (cm)		23.6 (6.3–147.7)
Seed activity (mCi)		0.6 (0.5–0.7)
Prescription dose (Gy)		150 (130–160)

and the tumor. If there was an error, real-time adjustments were made according to the actual image.

Puncture and seed implantation

After 3DPT was aligned exactly, the seed needle was moved to a predetermined depth by percutaneous puncture through the template guide column. A CT scan was performed to verify the position of the seed needle during the puncture process, and fine-tuning was performed if necessary. Finally, the seeds were implanted based on the preoperative plan and the actual depth of each needle in the target zone. After the implantation was completed, the CT scan was performed again to observe the actual distribution of the seeds (whether they were uniform, whether there was falling off or shift, etc.). If there was a cold spot in the seed distribution, the seeds were re-implanted.

Postoperative dosimetric verification

A CT scan was performed after the operation. The images were transmitted to BTPS, and GTV and OAR were re-delineated. The dose obtained by GTV and OAR was calculated and evaluated according to the actual seed distribution. The technical flow of 3DPT combined with CT guided seed implantation was shown in Fig. 1.

CONSISTENCY ANALYSIS OF NEEDLE TRACK AND DOSE

Comparison of preoperative and intraoperative needle tracks

In BTPS, the final image after the intraoperative puncture needle was in place, fused and registered with the preoperative plan image. The registration mode used was bone rigid registration, to reduce the influence of tissue deformity, organ movement and respiration. On the fusion image, both the virtual needle track in the preoperative plan and the actual needle track were displayed (Fig. 2). The parameters of the two-needle tracks before and during the operation were compared. The indicators included the following: angle, depth, puncture point position and needle tip position. The needle angle was measured based on the default coordinate system of CT image (the positive direction of x-axis is 0°, the negative direction of x-axis is 180°, the positive direction of y-axis is 90° and the negative direction of y-axis is 270°). The angle between the needle path and the positive direction of x-axis was the needle angle (which can be automatically obtained by the BTPS). The length from the puncture point to the needle tip was the measured needle depth. The absolute value of the difference between the planned needle angle and the actual needle angle was directly measured as the error value of the needle angle. The absolute value of the difference between the planned needle depth and the actual needle depth was

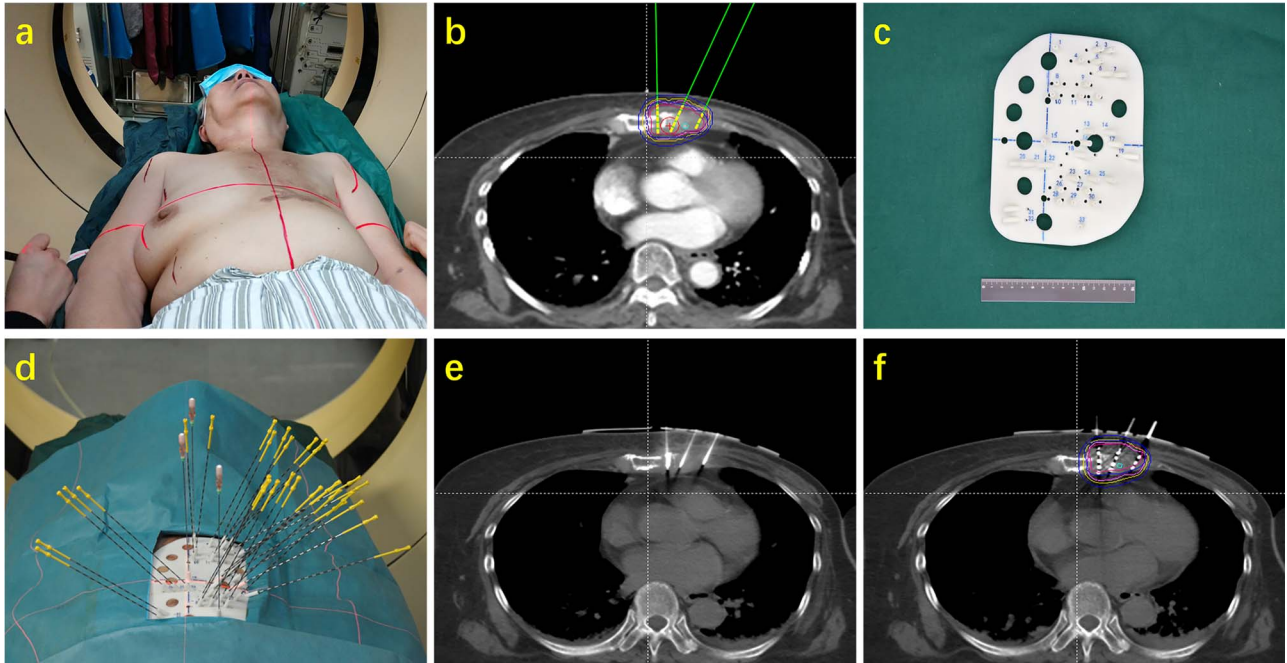


Fig. 1. Brief technical flow of 3DPT combined with CT guided seed implantation: a. Preoperative CT positioning; b. Preoperative planning design; c. The 3DPT design and printing; d. The 3DPT alignment and 3DPT guided needles insertion; e. CT monitoring needles position; f. CT monitoring seeds distribution and dosimetric verification.

directly measured as the error value of the needle depth. The distance between the planned puncture point and the actual puncture point was directly measured as the error value of the puncture point position. The distance between the planned needle tip and the actual needle tip was directly measured as the error value of the needle tip position.

Dosimetric comparison between pre-, intra- and post-operation

The preoperative, intraoperative and postoperative dosimetric parameters were compared, which included the following: D90 (dose received by 90% of GTV), V100, V150, V200 (volume percentage of GTV received 100%, 150% and 200% of the prescribed dose), and minimum peripheral dose (MPD; GTV received minimum marginal dose). The conformal index (CI) was used to evaluate the conformal degree of dose distribution [14]:

$$CI = (V_{T,ref}/V_T) \times (V_{T,ref}/V_{ref})$$

where, V_T , $V_{T,ref}$ and V_{ref} were the volume of the target zone, volume of the prescribed dose received by target zone and total volume (cm^3) contained in the prescribed dose, respectively, and wherein the ideal CI was 1. The external index (EI) described the percentage of the volume of the prescribed dose received outside the target to the volume of the target zone [15]:

$$EI = (V_{ref} - V_{T,ref}) / V_T \times 100\%$$

The most ideal EI value was 0. Homogeneity Index (HI) described the uniformity of dose distribution [15]:

$$HI = (V_{T,ref} - V_{T,1.5ref}) / V_{T,ref} \times 100\%$$

where $V_{T,1.5ref}$ was the volume of target zone receiving 150% of the prescribed dose (cm^3). The most ideal HI was 100%. The larger the HI, the more uniform the dose distribution in the target zone.

Comparison of other treatment parameters before, during and after the operation: indicators included GTV volume, number of needles, number of seeds, etc.

STATISTICAL METHODS

Statistical analysis was performed using statistical software SPSS 20.0 (IBM, Armonk, NY). The variables data were described by the mean \pm standard deviation. The attributes data were described by the absolute value and percentage (rate). First, the Shapiro–Wilk test was used to verify whether each group of data conformed to the normal distribution. For the data conforming to the normal distribution, the two groups were compared by the t-test. The multiple group comparison was performed by analysis of variance. For the data that did not conform to the normal distribution, the non-parametric test was used. The two groups were compared using the Wilcoxon test. Multiple group comparison was performed by the Friedman test. P-value < 0.05 was considered statistically significant.

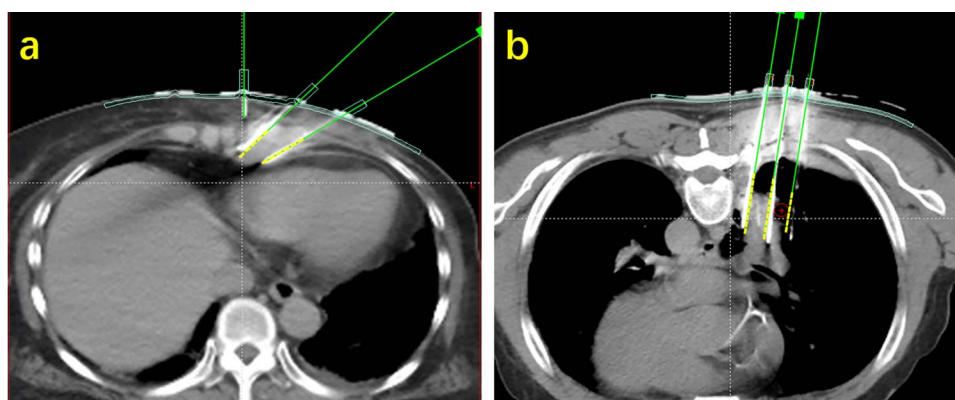


Fig. 2. There are errors between the actual needle track and the preoperative needle track: a. For chest wall lesions, the error is relatively small; b. For lung lesions, the error is relatively large, and the needle deviation in the cranial-caudal direction may occur.

Table 2. Comparison results of the actual needle angle and needle depth during the operation and those designed in the preoperative plan

Parameters	Preoperative		Intraoperative (actual)		Absolute value of error		p value
	Range	Mean \pm SD*	Range	Mean \pm SD*	Range	Mean \pm SD*	
Needle angle ($^{\circ}$)	2.8–175.1	93.2 \pm 38.76	3.4–177.2	92.6 \pm 38.17	0–8.9	2.8 \pm 1.73	0.023
Needle depth (cm)	3–13.9	8.1 \pm 2.52	2.9–13.28	8.3 \pm 2.45	0–3.1	0.52 \pm 0.48	<0.001

*SD, Standard Deviation

RESULTS

According to the established technical process, all patients successfully completed the 3DPT-assisted CT-guided RISI operation. A total of 318 needles were used in the entire study population. The number of needles used for cases involving the left lung, right lung and chest wall was 42, 194 and 82, respectively. The number of needles used in the upper and lower lung cases was 66 and 170, respectively.

Comparison of errors during needle tracking in the whole patient group

Table 2 presents the comparison results of the actual needle angle and needle depth during the operation and those designed in the preoperative plan. The actual angle and depth of needle insertion were different from those designed in the preoperative plan, with statistical significance ($P < 0.05$). In addition, the average value of the needle insertion point error was 3.4 ± 1.7 mm (range, 0–8.5 mm). The average value of needle tip error was 4.4 ± 2.9 mm (range, 0–25 mm).

Comparison of errors during needle tracking in different parts

Table 3 shows the error comparison results of the left lung, right lung and chest wall cases. Table 4 lists the error comparison results of the upper lobe, lower lobe and chest wall cases. Among them, the error value of chest wall cases was smaller than that of the left lung and right lung. These differences were statistically significant ($p < 0.05$). This was still in the case of comparing the chest wall and upper/lower lobes, while the error value of the chest wall case was lower than that

of the upper and lower lobes, with statistically significant differences ($p < 0.05$).

Comparison results of the parameters of pre-, intra- and postoperative plans

Table 5 shows the comparison results of the dosimetric parameters of the three groups of plans (preoperative, intraoperative and postoperative). There was no significant difference in the D90 values estimated in the postoperative plan when compared to with those estimated in the preoperative and intraoperative plans ($p > 0.05$). Compared with the preoperative plan, V100 of the postoperative plan was lower, V200 was higher, CI was lower and HI was higher. The differences were statistically significant ($p < 0.05$). Compared with the preoperative plan, V100 of the intraoperative plan was lower, V200 was higher, CI was lower, EI was higher and HI was higher, and the differences were statistically significant ($p < 0.05$). There was no statistical difference in the dosimetric parameters between the postoperative plan and the intraoperative plan ($p > 0.05$). In addition, the postoperative GTV volume was higher than that before and during the operation. The difference was statistically significant ($p < 0.05$).

DISCUSSION

RISI's template concept originated from prostate cancer [16]. However, because it was a coplanar design, it had great limitations when applied to other parts of the body. This is because in most cases it is usually difficult to perform multi-needle and coplanar puncture and

Table 3. Comparison of errors during needle tracking of cases involving the left lung, right lung and chest wall

Parameters	LL		RL		CC		p value		
	Range	Mean ± SD	Range	Mean ± SD	Range	Mean ± SD	LL/RL	LL/CW	RL/CW
Error of needle angle (°)	0–8.2	3.3 ± 2.1	0–8.9	2.8 ± 1.55	0.2–8	2.3 ± 1.53	0.062	0.001	0.027
Error of needle depth (cm)	0.01–1.47	0.35 ± 0.31	0–3.1	0.66 ± 0.53	0–1.21	0.29 ± 0.27	0.307	<0.001	<0.001
Error of needle entry point (mm)	0–8.5	4.3 ± 1.7	0–6.9	3.2 ± 1.7	0–5.5	2.9 ± 1.2	0.836	0.001	<0.001
Error of needle tip (mm)	1.6–9.3	4.4 ± 1.7	0–25	4.7 ± 3.4	0–6.2	3.0 ± 1.5	0.419	<0.001	0.001

SD, Standard Deviation; LL, Left Lung; RL, Right Lung; CW, Chest Wall.

Table 4. Comparison of errors during needle tracking of involving the upper lobe, lower lobe and chest wall

Parameters	UL		MLL		CW		p value		
	Range	Mean ± SD	Range	Mean ± SD	Range	Mean ± SD	UL/MLL	UL/CW	MLL/CW
Error of needle angle (°)	0.5–8.9	2.9 ± 1.35	0–8.2	2.6 ± 1.63	0.2–8	2.3 ± 1.53	0.062	0.001	0.027
Error of needle depth (cm)	0.02–3.10	0.54 ± 0.47	0–3.05	0.63 ± 0.53	0–1.21	0.29 ± 0.27	0.307	<0.001	<0.001
Error of needle entry point (mm)	0–8.5	4.3 ± 1.7	0–6.9	3.2 ± 1.7	0–5.5	2.9 ± 1.2	0.836	0.001	<0.001
Error of needle tip (mm)	0–14.4	5.1 ± 2.8	0–25	4.7 ± 3.4	0–6.2	3.0 ± 1.5	0.419	<0.001	0.001

SD, Standard Deviation; UL, Upper Lobe; MLL, Middle and Lower Lobe; CW, Chest Wall.

Table 5. Comparison results of various parameters in preoperative, intraoperative and postoperative plans

Parameters	Pre		Intra		Post		p value		
	Range	Mean ± SD	Range	Mean ± SD	Range	Mean ± SD	Intra/Pre	Intra/Post	Pre/Post
GTV volume (cm ³)	6.3–147.7	38.7 ± 38.62	7.1–149.6	37.7 ± 35.94	7.3–151.6	39 ± 36.63	0.006	0.004	0.006
Number of needles	4–36	13 ± 7	6–32	13 ± 6	-	-	0.165	-	-
Number of seeds	4–112	51 ± 28	5–115	53 ± 28	5–115	54 ± 28	0.101	0.257	0.04
D90 (Gy)	134.9–203.8	162.9 ± 17.29	109.8–207.1	159.3 ± 25.46	111.0–214.6	161.1 ± 27.24	0.21	0.672	0.635
MPD (Gy)	52.3–137.1	85.3 ± 22.84	37.6–136.3	80.6 ± 26.41	38.9–136.8	81.9 ± 23.14	0.466	0.776	0.577
V100 (%)	6.1–110.4	36.3 ± 30.73	6.7–106.7	35.8 ± 30.19	5.8–135.7	35.3 ± 6.22	0.031	0.904	0.049
V150 (%)	2.7–106.7	26.2 ± 26.30	3.6–96.1	27.4 ± 24.17	3.9–97.8	26.2 ± 23.94	0.108	0.492	0.13
V200 (%)	0.9–68.8	14.5 ± 16.30	1.7–72.8	17.2 ± 17.33	2.1–71.4	16.8 ± 16.90	0.008	0.64	0.002
CI	0.19–0.80	0.57 ± 0.155	0.17–0.83	0.51 ± 0.167	0.16–0.82	0.51 ± 0.178	0.009	0.841	0.016
EI (%)	0.14–3.51	0.79 ± 0.836	0.08–4.18	0.89 ± 0.957	0.08–3.71	0.83 ± 0.850	0.048	0.107	0.171
HI (%)	0.09–0.64	0.26 ± 0.129	0.11–0.69	0.31 ± 0.150	0.05–0.60	0.28 ± 0.132	0.003	0.259	0.05

SD, Standard Deviation; Pre, Preoperative; Intra, Intraoperative; Post, Postoperative.

implantation to avoid important structures. The 3DPT technology makes up for the insufficiency of the coplanar design [8, 17]. It not only enables individualized, non-coplanar and multi-angle complex puncture and implantation but also has good treatment accuracy, as shown by the results of this study. When combined with intraoperative optimization, it provides effective quality control and quality assurance for RISI.

This study suggests that although there are additional control measures such as negative pressure vacuum pads, positioning laser lines, template coordinate lines, etc., there are still errors in the template-guided RISI for chest lesions. The average distance error is within 6 mm, and the average angle error is within 3 degrees. Some studies

have analyzed the error during needle tracking in the application of 3DPT-guided RISI for head and neck tumors. The mean error during needle tracking is 5.2 mm [18]. Another study analyzed the error during needle tracking of 3DPT-guided RISI for retroperitoneal tumor. The errors in needlepoint, needle angle and needle tip are 4.5 ± 4.1 mm, $2.7 \pm 3.0^\circ$ and 6.9 ± 6.0 mm, respectively [19]. Although this study was performed on the chest, the error range was similar, and it was considered that the accuracy of the template-guided needle insertion was good.

The difference between the actual needle tracks in the whole group and those designed in the preoperative plan was statistically significant. The sources of error were considered as follows: (i) local anesthesia

caused changes in skin shape and thickness in the treatment area, and poor fit between the template and the body surface, (ii) errors in template alignment, (iii) there was squeezing during alignment of the normal tissue that the track passed through, (iv) respiratory and organ movement would cause changes in the position between the lesion and the template and puncture needle, (v) there was rib blocking in the local area of the lesion, causing the puncture needle to deviate from the predetermined track or deformation of the needle by force during the puncture, (vi) the printing accuracy of the template affected the accuracy of needle track control. At the same time, the error during needle tracking of chest wall lesions was smaller than that of the lungs. This was also considered to be related to the fact that the lesions were relatively fixed, there was no influence by respiratory movement, and there was no blockage caused by bones.

This study further analyzed the preoperative, intraoperative and postoperative dose display. The differences in some dosimetric indicators (V100, V200, CI, HI) of the preoperative and postoperative plans were statistically significant, however, the differences between the dosimetric indicators of the postoperative and intraoperative plans were not statistically significant. This indicates that due to the existence of errors, after real-time adjustment of the intraoperative plan, the postoperative dose could meet the requirements of the intraoperative plan. This also reminds us of the necessity of intraoperative optimization (planning). Through intraoperative optimization, the distribution of needles, seeds and dose can be brought closer to the actual situation during the operation. In addition, D90 is the main dose parameter for RISI treatment evaluation. When weighing various parameters, we give priority to meeting the requirements for D90. Therefore, D90 was consistent in preoperative, intraoperative and postoperative plans. At the same time, the dosimetric errors may also come from other factors: (i) operation errors would occur in the seed implantation stage, especially for osteoclastic lesions or lesions with liquefaction and necrosis, the actual needle removal distance and the number and distribution of seeds failed to be completely consistent with the preoperative plan, (ii) the consistency of the target zone would also affect the preoperative and postoperative dose distribution. The average postoperative GTV volume in this study increased relative to that estimated preoperatively (39 cm^3 vs 38.7 cm^3), the difference was statistically significant ($p = 0.006$) and was thought to be related to bleeding, edema and delineation errors.

Based on the causes of errors obtained from the above analysis, the solutions we propose to reduce errors include the following: (i) full local compression after anesthesia, which would not only promote the absorption of anesthetics but also reduce body surface deformity; (ii) when designing the template range, areas with relatively significant body surface features should be included for better accuracy and stability of the 3DPT alignment, (iii) the shortest implantation track should be selected to reduce the influence of deviation in needle insertion, (iv) a 4D-CT scan should be used to completely cover the movement area of the tumor, to provide information for the position of the reserved needles, (v) during the operation of seed implantation, the force of needles pulling and seeds pushing should be moderate to avoid changes in needles and seeds position. In addition, the printing accuracy of 3DPT is determined by three factors: CT image data accuracy, software design accuracy and manufacturing equipment accuracy [20]. The accuracy of computed 3D design software and 3D printing rapid prototyping

equipment has reached the micrometer or even nanometer level. Thus, the accuracy of the template mainly depends on the accuracy of the CT image data. In practical applications, we found that the thinner the slice thickness of the CT scan, the higher the accuracy of the printed template, but the 5 mm slice thickness scan can already meet the clinical needs in most cases, while for lesions less than 3 cm or areas where has higher requirements for implantation accuracy, and thin-slice scanning can be considered to improve template guidance accuracy.

CONCLUSION

The mean needle insertion error of 3DPT applied to chest tumor RISI is less than 6 mm. The error of chest wall lesions is less than that of the lung. The postoperative dose is slightly different from the preoperative dose. However, it can meet the dosimetric requirements of the intraoperative plan after intraoperative optimization. With the accumulation of operating experience and the optimization of operating details, reduction in errors and improvement in treatment accuracy is further expected.

CONFLICT OF INTEREST

The authors declare they have no conflicts of interest.

FUNDING

National Key Research and Development Program of China (2019YFB1311300, 2019YFB1311305).

Key Clinical Project of Peking University Third Hospital (BYSYZD2019010).

REFERENCES

1. Keyes M, Crook J, Morton G et al. Treatment options for localized prostate cancer. *Can Fam Physician* 2013;59:1269–74.
2. Meng N, Jiang YL, Wang JJ et al. Permanent implantation of iodine-125 seeds as a salvage therapy for recurrent head and neck carcinoma after radiotherapy. *Cancer Invest* 2012;30:236–42.
3. Wang ZM, Lu J, Liu T et al. CT-guided interstitial brachytherapy of inoperable non-small cell lung cancer. *Lung Cancer* 2011;74:253–7.
4. Wang H, Wang J, Jiang Y et al. The investigation of 125I seed implantation as a salvage modality for unresectable pancreatic carcinoma. *J Exp Clin Cancer Res* 2013;32:106–13.
5. Zhuang HQ, Wang JJ, Liao AY et al. The biological effect of 125I seed continuous low dose rate irradiation in CL187 cells. *J Exp Clin Cancer Res* 2009;28:12–20.
6. Rembowska AME, Cook M, Hoskin PJ et al. The stepping source dosimetry system as an extension of the manchester system. *Radiotherapy & Oncology* 1996;39:S25.
7. Nath R, Bice WS, Butler WM et al. AAPM recommendations on dose prescription and reporting methods for permanent interstitial brachytherapy for prostate cancer: Report of Task Group 137. *Med Phys* 2009;36:5310–22.

8. Ji Z, Jiang Y, Guo F et al. Dosimetry verification of radioactive seed implantation for malignant tumors assisted by 3D printing individual templates and CT guidance. *Applied Radiation and Isotopes* 2017;124:68–74.
9. Wang H, Peng R, Li X et al. The dosimetry evaluation of 3D printing non-coplanar template-assisted CT-guided 125I seed stereotactic ablation brachytherapy for pelvic recurrent rectal cancer after external beam radiotherapy. *Journal of Radiation Research* 2021;62:473–82.
10. Ji Z, Sun H, Jiang Y et al. Comparative study for CT-guided (125)I seed implantation assisted by 3D printing coplanar and non-coplanar template in peripheral lung cancer. *J Contemp Brachytherapy* 2019;11:169–73.
11. Nath R, Anderson LL, Luxton G et al. Dosimetry of interstitial brachytherapy sources: recommendations of the AAPM Radiation Therapy Committee Task Group No. 43. American Association of Physicists in Medicine. *Med Phys* 1995;22:209–34.
12. Rivard MJ, Coursey BM, DeWerd LA et al. Update of AAPM Task Group No. 43 Report: A revised AAPM protocol for brachytherapy dose calculations. *Med Phys* 2004;31:633–74.
13. Wang J, Chai S, Zheng G et al. Expert consensus statement on computed tomography-guided (125)I radioactive seeds permanent interstitial brachytherapy. *J Cancer Res Ther* 2018;14:12–7.
14. van't Riet A, Mak AC, Moerland MA et al. A conformation number to quantify the degree of conformality in brachytherapy and external beam irradiation: application to the prostate. *Int J Radiat Oncol Biol Phys* 1997;37:731–6.
15. Saw CB, Suntharalingam N. Quantitative assessment of interstitial implants. *Int J Radiat Oncol Biol Phys* 1991;20:135–9.
16. Nath S, Chen Z, Yue N et al. Dosimetric effects of needle divergence in prostate seed implant using 125I and 103Pd radioactive seeds. *Medical Physics* 2000;27:1058–66.
17. Huang MW, Liu SM, Zheng L et al. A digital model individual template and CT-guided 125I seed implants for malignant tumors of the head and neck. *J Radiat Res* 2012;53:973–7.
18. Zhang GH, Lv XM, Wu WJ et al. Evaluation of the accuracy of computer-assisted techniques in the interstitial brachytherapy of the deep regions of the head and neck. *Brachytherapy* 2019;18:217–23.
19. Jiang W, Jiang P, Wei S et al. The accuracy and safety of CT-guided iodine-125 seed implantation assisted by 3D non-coplanar template for retroperitoneal recurrent carcinoma. *World J Surg Oncol* 2020;18:307–14.
20. Zhao Y, Wang Y, Huang M et al. Computer aided design method of digital individual guide for brachytherapy. *Zhonghua Kou Qiang Yi Xue Za Zhi* 2014;49:115–8.